

Electromagnetic Imaging by the Genetic Algorithm

Wei Chan, Ching-Lieh Li and Chien-Ching Chiu

Abstract-The genetic algorithm is used to reconstruct the shapes of two perfectly conducting cylinders. Bases on the boundary condition and the measured scattered field, a set of nonlinear integral equations is derived and the imaging problem is reformulated into an optimization problem. The genetic algorithm is then employed to find out the global extreme solution of the cost function. Numerical examples are given to demonstrate the capability of the inverse algorithm. Good reconstruction is obtained even when the multiple scattering between two conductors is serious. In addition, the effect of Gaussian noise on the reconstruction results is investigated.

I. INTRODUCTION

The inverse scattering problem of conducting objects has been a subject of considerable importance in noninvasive measurement and remote sensing. In the past 20 years, many rigorous methods have been developed to solve the exact equations [1-3]. However, inverse problems of this type are difficult to solve because they are illposed and nonlinear. As a results, many inverse problem are reformulated as optimization problems. The optimization problems are numerically solved by different iterative methods such as the Newton-Kantorovitch method [1], the Levenberg-Marquardt algorithm [2], and the successive-overrelaxation method [3]. However these approaches apply the gradient search method to find the extreme of the cost function which are highly dependent on the initial guess and tends to get trapped in a local extreme. In this article, we present a method based on the genetic algorithm to recover the shape of two separate perfectly conducting cylinders illuminated by transverse magnetic (TM) waves. The genetic algorithm [4] is a well-known algorithm that uses the stochastic random choice to search through a coding of a parameter space. Compared to gradient search optimization techniques, the genetic algorithm is less prone to convergence to a local minimum, which in turn renders it an ideal candidate for global optimization. It usually converges to the global extreme of the problem, no matter what the initial is [4].

Manuscript Received on April 18, 1999. This work was supported by the National Science Council, Republic of China, Grant NSC 85-2213-E032-001.

The authors are with the Department of Electrical Engineering, Tamkang University, Tamsui, Taiwan, ROC. Email:chiu@ee.tku.edu.tw Fax: 886-2-26221565

II. THEORETICAL FORMULATION

Let us consider two separate perfectly conducting cylinders with cross section described in polar coordinates in xy plane by the equations $\rho_1 = F_1(\theta_1)$ and $\rho_2 = F_2(\theta_2)$ centered at $(d_1 \cos \psi, d_1 \sin \psi)$ and $(-d_2 \cos \psi, -d_2 \sin \psi)$, respectively, in free space. Let (ϵ_0, μ_0) denote the permittivity and permeability respectively of free space. A plane wave whose electric field vector is parallel to z-axis (i.e., transverse magnetic or TM polarization) is incident upon the scatterers. We assume that the time dependence of the field is harmonic

with the factor $\exp(j\omega t)$. Let \vec{E}_i denote the incident field with incident angle ϕ , as shown in Fig. 1. Then the incident field is given by

$$\vec{E}_i(x, y) = e^{-jk(x \sin \phi + y \cos \phi)} \hat{z},$$
$$k^2 = \omega^2 \epsilon_0 \mu_0. \quad (1)$$

At an arbitrary point (x,y) in Cartesian coordinates outside the scatterers, the scattered field, $\vec{E}_s = \vec{E} - \vec{E}_i$, can be expressed by (2)

and $H_0^{(2)}$ is the Hankel function of the second kind of order zero, and $J_{,i}(\theta_i)$ is the induced surface current density which is proportional to the normal derivative of electric field on the *i*th conductor surface.

The boundary condition states that the total tangential electric field at the surface of the scatterers must be zero and this yields two integral equations for $J_1(\theta_1)$ and $J_2(\theta_2)$: (3) and (4) respectively. For the direct scattering problem, the scattered field E_s is calculated by assuming that the positions and the shapes of the objects are known. This can be achieved by first solving J_1 and J_2 in (3) and (4) and calculating E_s in (2). Next, let us consider the following inverse problem: given the scattered field E_s measured outside the scatterers, determine the shapes $F_1(\theta_1)$ and $F_2(\theta_2)$ of the objects. Assume the approximate center of the scatterer is known.

$$E_s(x, y) = - \int_0^{2\pi} \frac{j}{4} H_0^{(2)} [k \sqrt{(x_1 - F_1(\theta') \cos \theta')^2 + (y_1 - F_1(\theta') \sin \theta')^2}] J_1(\theta') d\theta' \quad (2)$$

$$- \int_0^{2\pi} \frac{j}{4} H_0^{(2)} [k \sqrt{(x_2 - F_2(\theta') \cos \theta')^2 + (y_2 - F_2(\theta') \sin \theta')^2}] J_2(\theta') d\theta'$$

with

$$J_i(\theta_i) = -j\omega\mu_0 \sqrt{F_i^2(\theta_i) + F_i'^2(\theta_i)} J_{si}(\theta_i), \quad i=1,2$$

$$(x_1, y_1) = (x - d_1 \cos \psi, y - d_1 \sin \psi),$$

$$(x_2, y_2) = (x + d_2 \cos \psi, y + d_2 \sin \psi),$$

$$E_i(F_1(\theta_1) \cos \theta_1 + d_1 \cos \psi, F_1(\theta_1) \sin \theta_1 + d_1 \sin \psi) = \quad (3)$$

$$\int_0^{2\pi} \frac{j}{4} H_0^{(2)}(kr_{01}) J_1(\theta') d\theta' + \int_0^{2\pi} \frac{j}{4} H_0^{(2)}(kr_{03}) J_2(\theta') d\theta'$$

$$E_i(F_2(\theta_2) \cos \theta_2 - d_2 \cos \psi, F_2(\theta_2) \sin \theta_2 - d_2 \sin \psi) = \quad (4)$$

$$\int_0^{2\pi} \frac{j}{4} H_0^{(2)}(kr_{04}) J_1(\theta') d\theta' + \int_0^{2\pi} \frac{j}{4} H_0^{(2)}(kr_{02}) J_2(\theta') d\theta'$$

where

$$r_{0i}(\theta_i, \theta') = \sqrt{[F_i(\theta_i) \cos \theta_i - F_i(\theta') \cos \theta']^2 + [F_i(\theta_i) \sin \theta_i - F_i(\theta') \sin \theta']^2}, \quad i=1,2$$

$$r_{03}(\theta_1, \theta') = \sqrt{[F_1(\theta_1) \cos \theta_1 - F_2(\theta') \cos \theta' + d \cos \psi]^2 + [F_1(\theta_1) \sin \theta_1 - F_2(\theta') \sin \theta' + d \sin \psi]^2}$$

$$r_{04}(\theta_2, \theta') = \sqrt{[F_2(\theta_2) \cos \theta_2 - F_1(\theta') \cos \theta' - d \cos \psi]^2 + [F_2(\theta_2) \sin \theta_2 - F_1(\theta') \sin \theta' - d \sin \psi]^2}$$

$$d = d_1 + d_2$$

Then the shape functions $F_1(\theta_1)$ and $F_2(\theta_2)$ can be expanded as:

$$F_1(\theta) = \sum_{n=0}^{N/2} B_{1n} \cos(n\theta) + \sum_{n=1}^{N/2} C_{1n} \sin(n\theta) \quad (5)$$

$$F_2(\theta) = \sum_{n=0}^{N/2} B_{2n} \cos(n\theta) + \sum_{n=1}^{N/2} C_{2n} \sin(n\theta)$$

where B_{1n} , C_{1n} , B_{2n} and C_{2n} are real coefficients to be determined, and $2^*(N+1)$ is the number of unknowns. In the inversion procedure, the genetic algorithm is used to minimize the following cost function express by (6):

$$CF = \left\{ \frac{1}{M_t} \sum_{m=1}^{M_t} \left| E_s^{\text{exp}}(\vec{r}) - E_s^{\text{cal}}(\vec{r}) \right|^2 / \left| E_s^{\text{exp}}(\vec{r}) \right|^2 + \alpha [|F_1'(\theta_1)|^2 + |F_2'(\theta_2)|^2] \right\}^{1/2} \quad (6)$$

where M_t is the total number of measurement points, and

$E_s^{\text{cal}}(\vec{r})$ and $E_s^{\text{exp}}(\vec{r})$ are the calculated scattered field and the measured scattered field, respectively. Note that the regularization term $\alpha [|F_1'(\theta_1)|^2 + |F_2'(\theta_2)|^2]$ was added in equation (6). The minimization of $\alpha [|F_1'(\theta_1)|^2 + |F_2'(\theta_2)|^2]$ can, to a certain extent, be interpreted as the smoothness requirement for the boundary of $F_1(\theta_1)$ and $F_2(\theta_2)$. Therefore, the minimization of CF can be interpreted as the minimization of the least-squares error between the measured and the calculated fields with the constraint of a smooth boundary. Typical values of α range from 0.0001 to 10; but ideally, it is decreased as the convergence has been attained [3]. The optimal value of α is mostly dependent on the dimensions of the geometry. One can always choose a large enough value to ensure the

convergence, although overestimation will result in a very smooth reconstruction [1]. For numerical calculation of the problem, the contour of the object is first divided into sufficient small segments so that the induced surface current can be considered constant over each segment. Then the moment method is used to solve Equations (2), (3) and (4) with the pulse basis functions for expanding, and the Direct delta function for testing. Genetic algorithms are the global numerical optimization methods based on genetic recombination and evaluation in nature [6]. They use the iterative optimization procedures that start with a randomly selected population of potential solutions, and then gradually evolve toward a better solution through the application of

the genetic operators. Genetic algorithms typically operate on a discretized and coded representation of the parameters rather than on the parameters themselves. These representations are often considered to be "chromosomes," while the individual element that constitutes the chromosome representations for optimization problem involving several continuous parameters can be obtained through the juxtaposition of discretized binary representations of the individual parameters. In our problem parameters B_{1n} , C_{1n} , B_{2n} and C_{2n} are given by the following equation:

$$\xi = p_{\min} + \frac{p_{\max} - p_{\min}}{2^L - 1} \sum_{i=0}^{L-1} b_i^\xi 2^i \quad (7)$$

where ξ represents B_{1n} , C_{1n} , B_{2n} or C_{2n} . The b_0^ξ , $b_1^\xi, \dots, b_{L-1}^\xi$ (gene) is the L-bit string of the binary representation of B_{1n} , C_{1n} , B_{2n} or C_{2n} , and p_{\min} and

p_{\max} are the minimum and the maximum values admissible for B_{1n} , C_{1n} , B_{2n} and C_{2n} , respectively. The total unknown coefficients in Equation (7) would then be described by an $2(N+1)*L$ bit string (chromosome). The basic GA for which a flowchart is shown in Figure 2 starts with a large population containing a total of M candidates. Each candidate is described by a chromosome. Then the initial population can simply be created by taken M random chromosomes. Finally the GA iteratively generates a new population which is derived from the previous population through the application of the reproduction, crossover, and mutation operators.

III. NUMERICAL RESULTS

To demonstrate the capability of the present approach, two different examples are studied in our simulation. We consider two perfectly conducting cylinders in a free space, and a TM polarization plane wave is incident on the object as shown in Fig. 1. The frequency of the incident wave is set to be 3 GHz, i.e., the wavelength λ is 0.1m. Our intention is to reconstruct the shape of the object by using the scattered field measured outside. To reconstruct the shape of the cylinders, the object is illuminated by four incident waves with the incident angles of $\phi=0^\circ, 90^\circ, 180^\circ$, and 270° , and the measurement is taken on a circle of radius 7m at equal spacing. Note that for each incident angle, eight measurement points in each simulation. The number of unknowns is set to be 10. The population size is chosen as 300 (i.e. $M=300$). The crossover probability p_c and mutation probability p_m are set to be 0.8 and 0.1, respectively. The value of α is chosen to be 0.001. In the first example, $d_1=0.04$ and $d_2=0.08$ and ψ is 45° . The two shape functions are chosen to be $F_1(\theta_1)=(0.026+0.009\cos(2\theta_1))m$ and $F_2(\theta_2)=(0.03+0.0035\cos(2\theta_2)+0.0035\sin(2\theta_2))m$, respectively. The binary string length of the unknown coefficient, B_{1n} , C_{1n} , B_{2n} and C_{2n} , is set to be 8 bits (i.e. $L=8$). In other words, the bit number of a chromosome is 80 in case 1. The search range for the unknown coefficient of the shape function is chosen to be from 0. to 0.1. The extreme value of the coefficient of the shape function can be determined by the prior knowledge of the objects. With all these parameters, the reconstructed shape function is plotted in Fig. 3. It is clear that the reconstruction of the shape function is very good. Moreover, the error for the best population member (chromosome) is also shown. Note that the shape function of the initial generation is far from the exact one. To investigate the sensitivity of the imaging algorithm against random noise, two independent Gaussian noises with zero mean have been added to the real and imaginary parts of the simulated scattered fields. Normalized standard deviations of 10^{-5} , 10^{-4} , 10^{-3} , 10^{-2} and 10^{-1}

are used in the simulations. The normalized standard deviation mentioned earlier is defined as the standard deviation of the Gaussian noise divided by the rms value of the scattered fields. Here, the signal-to-noise ratio (SNR) is inversely proportional to the normalized standard deviation. The numerical result for this example is plotted in Figure 5. It is understood that the effect of noise is negligible for those normalized standard deviations that we below 10^{-2} . In the second example, the shape function is chosen to be $F_1(\theta_1)=(0.03+0.0025\cos(\theta_1)+0.005\cos(2\theta_1)+0.005\cos(3\theta_1))m$ and $F_2(\theta_2)=(0.03+0.005\sin(3\theta_2))m$. The parameters R , ψ , d_1 and d_2 are chosen as 7m, 135° , 0.08m and 0.07m respectively. The coding length and the search ranges for the unknown coefficients of the shape function are the same as in example 1. Again, with this set of parameter, satisfactory results are obtained in Fig. 4. This example implies that good reconstruction can be obtained when the scatterers are complex.

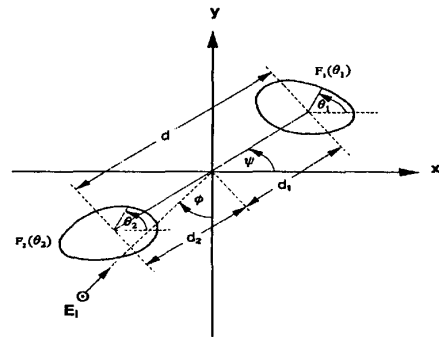


Fig. 1 The geometry in the (x,y) plane

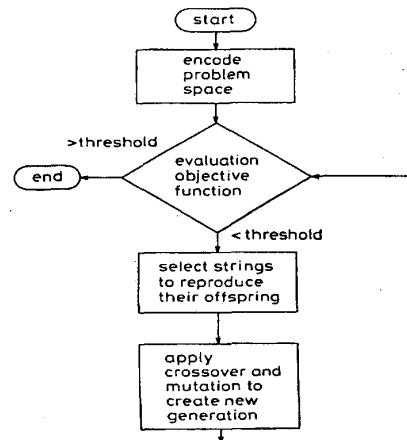


Fig. 2 The flowchart of Genetic Algorithm

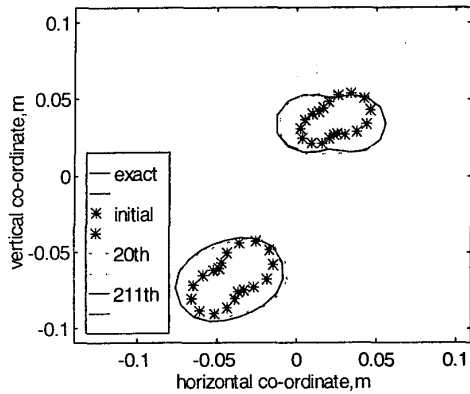


Fig. 3(a) The shape of example 1

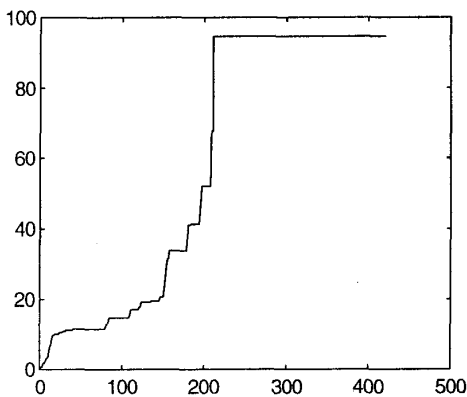


Fig.3 (b) The fitness of example 1

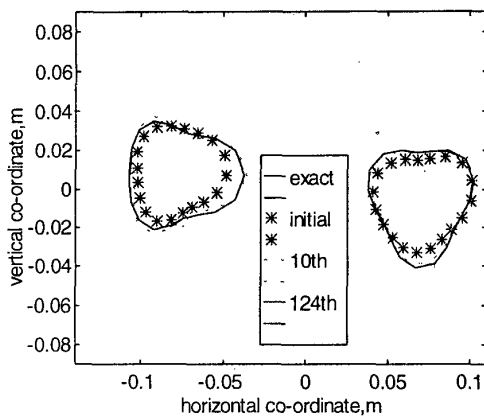


Fig.4 The shape of example 2

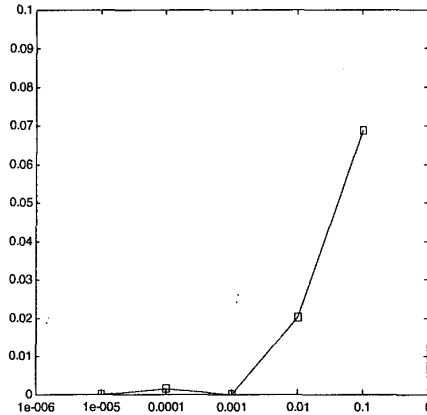


Fig. 5 The SNR of example 1.

IV. CONCLUSIONS

We have presented a study of applying the genetic algorithm to reconstruct the shapes of multiple conducting cylinders illuminated by TM waves. Based on the boundary condition and measured scattered field, we have derived a set of nonlinear integral equations and reformulated the imaging problem into an optimization problem. By using the genetic algorithm, the shape of the objects can be reconstructed. According to our experience, the main difficulties in applying the genetic algorithm to this problem are how to choose the parameters, such as the population size (M), bit length of the string (L), crossover probability (p_c), and mutation probability (p_m). Different parameter sets will affect the speed of convergence as well as the computing time required. From the numerical simulation, it is concluded that a population size from 300 to 600, a string length from 8 to 16 bits, with p_c and p_m in ranges of $0.7 < p_c < 0.9$ and $0.05 < p_m < 0.15$ are suitable for imaging problems of this type.

REFERENCES

1. C.C.Chiu and Y.W.Kiang, "Microwave imaging of multiple conducting cylinders," IEEE Trans. Antennas Prop. 40, 933-941 (1992).
2. F.Hettlich, "Two methods for solving an inverse conductive scattering problem," Inverse Problems 10, 375-385 (1994).
3. R.E.Kleinman and P.M. van den Berg, "Two-dimensional location and shape reconstruction," Radio Sci. 29, 1157-1169 (1994).
4. D.E.Goldberg, Genetic Algorithm in Search, Optimization and Machine Learning (Addison-Wesley), 1989.